ChemComm

ROYAL SOCIETY OF CHEMISTRY

COMMUNICATION

View Article Online
View Journal | View Issue

Cite this: *Chem. Commun.*, 2014, **50**, 9003

Received 15th May 2014,
Accepted 18th June 2014

DOI: 10.1039/c4cc03687e

www.rsc.org/chemcomm

Concentration dependent halogen-bond density in the 2D self-assembly of a thienophenanthrene derivative at the aliphatic acid/graphite interface†

Bao Zha, Xinrui Miao,* Pei Liu, Yumeng Wu and Wenli Deng*

The supramolecular patterns of a thienophenanthrene derivative could be switched among dissimilar polymorphs with different halogen-bond densities by solution concentration, which is demonstrated through a combination of STM and density functional theory (DFT) calculations.

Rational molecular design and external condition change (such as solvent, concentration and temperature) are considered as powerful approaches to tune the ordered pattern and structural transformation at the molecular scale for two-dimensional (2D) self-assembly.[1] Many different nanostructures for alkyl chain substituted molecules have been fabricated involving van der Waals force,[2] hydrogen bonding,[3] dipolar interaction,[4] *etc.* Very recently, halogen bonding has been used to achieve the formation of self-assembled patterns for organic molecules, because it is expected to be highly directional, and its binding geometry can adopt a few configurations.[5] These characteristics provide new opportunities for tailing molecular self-assembly and therefore obtaining novel nanopatterns by scanning tunneling microscopy (STM). However, reports describing the formation of 2D halogen-bonded structures on solid surfaces mainly focus on the rigid molecules.[6] As far as we know, the application of halogen bonding in the 2D self-assembly of alkyl chain and bromine substituted organic molecules at the solid–liquid interface has not been investigated by STM widely. In addition to the intermolecular interaction, the solvent can drastically affect the structure of halogen-bonded architectures at the solid–liquid interfaces.[7] The influence of the solution concentration on halogen-bond density of 2D self-assembly of alkyl chain and bromine substituted organic building blocks at the solid–liquid interface still remains obscure.

Herein we present the first case of the competition of halogen bonding and van der Waals interaction on the self-assembly of DDTD at the aliphatic acid/graphite interface using STM. It was found that different nanostructures could be formed by adjusting the DDTD concentration. In addition, the voltage pulse applied to the STM tip could induce the structural transformation. All the conjugated moieties of DDTD appear to be triangle features in the STM images. Our systematic study illustrates that the competition of interchain van der Waals interactions and halogen bonding of the Br···Br and Br···H bonds along with solvent coadsorption determine the polymorphous structures. The present work provides a molecular insight into the 2D assembly of a thienophenanthrene derivative based on halogen bonding.

The DDTD molecule with optical properties (Fig. S1, ESI†) was home-synthesized (Fig. 1a and ESI†). The calculated electrostatic potential of a single DDTD and a dimer is shown in Fig. 1b and c. Since Br has both positive and negative electrostatic parts, the positive potential region could point toward the negative part of the other Br atom. Therefore, two DDTD molecules are doubly bonded by Br···Br and Br···H pairs (Fig. 1c), resulting in a triangular motif. Electrostatic interactions are identified as the driving forces for intermolecular Br···Br and Br···H bonding.

A drop of saturated solution of DDTD was applied to a freshly cleaved graphite surface under ambient conditions (15 °C). An assembly which we called an alternate pattern occurs fast and mostly covers the whole area (Fig. 2a and Fig. S2, ESI†). In adjacent one-row molecular lamellae, the conjugated cores arrange in an antiparallel mode as the blue arrows indicate in Fig. 2a. The antiparallel alignment of the molecular dipoles is a consequence of stabilizing

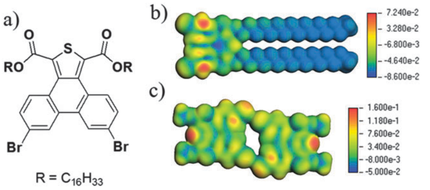

Fig. 1 (a) Chemical structure of DDTD. (b) Calculated electrostatic potential map of DDTD under vacuum. (c) Electrostatic potential map of the DDTD dimer under vacuum showing the transformation of charge due to dispersion and electrostatic forces of the halogen bonds.

College of Materials Science and Engineering, South China University of Technology, Guangzhou, 510640 China. E-mail: msxrmiao@scut.edu.cn, wldeng@scut.edu.cn; Tel: +86 20-22236708

† Electronic supplementary information (ESI) available: STM experimental conditions, synthesis and characterization of DDTD and DPTD, additional STM images and packing parameters and binding energy calculation. See DOI: 10.1039/c4cc03687e

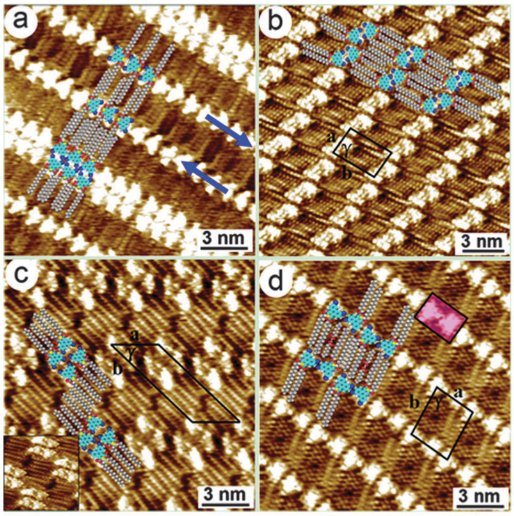

Fig. 2 STM images of the DDTD adlayers in 1-octanoic acid. (a) Alternate pattern (1.1 × 10^{-3} M). (b) Dislocated linear pattern (10^{-3}–10^{-5} M). (c) Tetramer structure (10^{-4}–10^{-5} M). Inset shows the halogen bonding of the tetramer. (d) Linear pattern (3.4 × 10^{-5} M). V_{bias} = 500–600 mV, I_t = 400–450 pA. Schematic representations of DDTD overlayed on each image to illustrate the molecular arrangements.

dipole–dipole forces, which govern the 2D structure formation.[8] Only in such lamellae the side chains of DDTD stretch on both sides of the conjugated core and interdigitate with those of neighboring molecules. In the two-row molecular lamellae, the DDTD molecules pack in a head-to-head fashion *via* Br···Br and Br···H interactions.

With the decreasing concentration, the alternate pattern disappeared gradually and a dislocated linear pattern and a tetramer pattern were observed (Fig. 2b and c). In Fig. 2b, two DDTD molecules form a dimer and arrange in a dislocated head-to-head fashion *via* a pair of halogen bonds. In each dimer, the alkyl chains of two DDTD molecules pack in the opposite direction. In Fig. 2c, four DDTD molecules arrange head-to-head, resulting from three pairs of halogen bonds. The side chains in adjacent lamellae arrange in a tail-to-tail fashion, indicating the stronger halogen bonding between the conjugated cores compared with the alternate and dislocated linear patterns.[9] When the DDTD concentration was decreased to 3.4 × 10^{-5} M, only the linear pattern was observed (Fig. 2d). Two DDTD molecules form a dimer according to a single halogen bond. Two solvent molecules forming a dimer with a head-to-head motif *via* hydrogen bonding coadsorb with DDTD due to the space matching as the superimposed molecular model shown in Fig. 2d.

The surface phases show clear concentration dependence (Fig. S3, ESI†): in the saturated solution (1.1 × 10^{-3} M), the alternate and dislocated linear patterns show phases separate on the surface (Fig. S4a, ESI†). In the concentration range (10^{-3}–10^{-5} M), the alternated pattern disappeared gradually and the dislocated linear and tetramer patterns coexist, in which the percentage of the tetramer pattern increases gradually (Fig. S4b–4d, ESI†). At the low concentration (3.4 × 10^{-5} M), only the linear pattern was formed resulting from the coadsorption of DDTD and 1-octanoic acid (Fig. S5, ESI†). Consecutive STM images (Fig. S6, ESI†) display the assembled pattern changing from an alternate motif to a dislocated linear pattern, which is driven by the change in the van der Waals force and halogen bonding. Compared with extensively studied hydrogen bonding, Br···Br and Br···H halogen bonding is weaker in energy which leads to faster dissociation dynamics.[6a] The phase transition was not observed between the dislocated linear pattern and the tetramer structure (Fig. S7, ESI†). The relative occurrence of three phases and structural transition on the surface reflects that at low concentrations, the dislocated linear pattern and the tetramer structure are the stable arrangements, whereas the alternate pattern is a stable phase at high concentrations. In the linear pattern, the coadsorption of solvent enhances the adlayer stability.

At the 1-heptoic acid or 1-nonoic acid/graphite interface, the alternate, dislocated linear and tetramer patterns are observed (Fig. S8 and S11, ESI†), which are similar to those in 1-octanoic acid. Moreover, the structural transition was recorded at high concentrations (Fig. S9, S10 and S12, ESI†). However, at low concentrations, another matrix pattern was obtained (Fig. 3 and Fig. S13, ESI†), in which no solvent molecule coadsorbs. The systematic results indicate that the solvent polarity affects the proportion of different structures (Fig. S8e and S11e, ESI†) and the amount of solvent is important for the formation of a coadsorbed structure.

In order to confirm the crucial role of halogen bonding in the structural polymorph of DDTD, the DPTD without the bromine atoms was home-synthesized (ESI†). The packing details show the conjugated cores of DPTD displaying triangle features arranged in pairs in a helix fashion and give a windmill-shaped tetramer as the green rectangles indicate in Fig. 4. Since the side chains interdigitate and lie along the graphite lattices (Fig. S14, ESI†), it can be inferred that the featured adlayer is influenced by the maximized molecule–substrate interaction. No solution concentration-dependence was observed (Fig. S15, ESI†). The results demonstrate that the self-assembled structure of DPTD is mainly dominated by the interchain van der Waals force and shape complementarity of cores. Compared with the self-assembly of DPDT, the halogen bonding plays an important role in the structural formation and transformation of DDTD.

It is commonly known that the concentration dependence is directly related to the difference in stability of different polymorphs and their respective molecular density. In principle, high-density structures are optimal from a free-energy point of view.

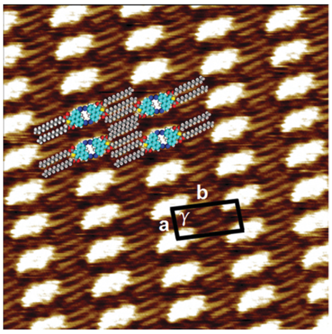

Fig. 3 STM image (17 × 17 nm^2) of the DDTD adlayer in 1-heptoic acid at a low concentration (2.5 × 10^{-5} M). V_{bias} = 600 mV, I_t = 400 pA.

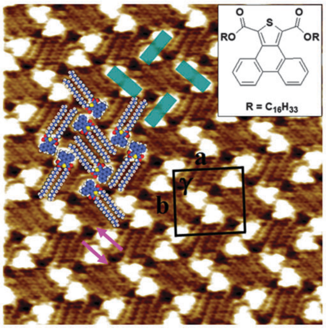

Fig. 4 High-resolution STM image (16×16 nm^2) of the DPTD adlayer at the 1-octanoic acid/graphite interface. V_{bias} = 570 mV, I_t = 420 pA.

The calculated molecular densities of the alternate, dislocated linear, tetrameric and linear patterns are 3.13, 3.75, 3.75 and 4.50 nm^2 per molecule, respectively (Table S1, ESI†). In our system, the alternate pattern with the highest packing density is thermodynamically stable in saturated solution. In all the phases, the side chains of DDTD molecules lie along the graphite lattice (Fig. S16, ESI†), indicating the same molecule–substrate interactions. However, only the side chains in adjacent lamellae are interdigitated in the alternate pattern, which illustrates the strongest intermolecular van der Waals interactions. With deceasing concentration, the DDTD molecules form a dimer or a tetramer, in which the coupled halogen bonds enhance the intermolecular interactions. When the carbon atom number of DDTD side chains is decreased down to 14, only the alternate pattern was obtained at different concentrations (Fig. S17 and S18, ESI†). The results demonstrate that the van der Waals interaction between the side chains and halogen bonding between the bromine atoms for DDTD adlayers either compete or cooperate in constructing polytypic intermolecular structures.

We performed DFT calculations to gain deeper insights into the intermolecular binding mechanisms within the adlayers. The molecular aggregations are stabilized by the Br···Br···H triangular structure between neighboring molecules, which has been observed in 3D crystal structures of other halogenated molecules.[10] Besides the van der Waals interaction between the side chains, the intermolecular halogen bonding plays an important role in the self-assembly of DDTD. The C–Br···Br angles α1 and α2 in dislocated and tetrameric patterns are about 90° and 180°, which are understood as charge-polarization induced halogen bonds. While α1 and α2 in the linear structure are the same indicating that the halogen bond is of the van der Waals type (Fig. 5 and Fig. S19, ESI†).[7,11] The calculated binding energies for dislocated, tetrameric and linear structures are −0.32, −0.96, and −0.11 eV, respectively (Fig. 5 and Fig. S20, ESI†). The binding energy of the tetramer is three times that of the dimer, indicating that two halogen bonds exist between the dimers. In the linear structure, only one halogen bond between two molecules results in two nonplanar molecules under vacuum. Considering the molecule–substrate and molecule–solvent interactions, such a pattern is also stable and all molecules are coplanar on the surface.

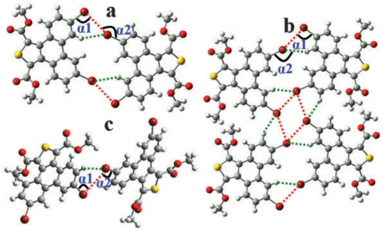

Fig. 5 Atomic structure of (a) dislocated, α1 ≈ 90°, α2 ≈ 180°, (b) tetrameric, α1 ≈ 90°, α2 ≈ 180° and (c) linear configuration obtained (α1 = α2) from DFT calculations. Dotted lines indicate possible intermolecular bonds, Br···Br (red) and Br···H (green).

In summary we have succeeded in controlling the halogen-bond density of DDTD at the 1-octanoic acid/graphite interface by changing the solution concentration. Four different molecular structures – alternate, dislocated linear, tetrameric, and linear – were observed. Based on the STM images, the proposed molecular models are in good agreement with the DFT calculations, and can be explained by a triangular structure consisting of the Br···Br and Br···H bonds. Without the solvent coadsorption, the higher the halogen-bond density, the more stable the structure is. The DDTD molecule has long side chains and Br atoms, so the van der Waals interactions of molecule–molecule and halogen bonding of the Br···Br and Br···H bonds along with solvent coadsorption determine the polymorphous structures. Our results open up new opportunities for tailoring molecular self-assembly by changing the intermolecular van der Waals interaction and halogen bonding. We will further investigate the position of halogen atoms, chain-length and solvent effects on the 2D molecular self-assembly.

Financial support from the National Program on the Key Basic Research Project (2012CB932900), the National Natural Science Foundation of China (21103053, 51373055) and the Fundamental Research Funds for the Central Universities (SCUT) is gratefully acknowledged.

Notes and references

1 (*a*) S. S. Jester, E. Sigmund and S. Höger, *J. Am. Chem. Soc.*, 2011, **133**, 11062; (*b*) T. Balandina, M. W. van der Meijden, O. Ivasenko, D. Cornil, J. Cornil, R. Lazzaroni, R. M. Kellogg and S. De Feyter, *Chem. Commun.*, 2013, **49**, 2207; (*c*) W. Mamdouh, H. Uji-i, J. S. Ladislaw, A. E. Dulcey, V. Percec, F. C. De Schryver and S. De Feyter, *J. Am. Chem. Soc.*, 2006, **128**, 317; (*d*) X. Zhang, T. Chen, Q. Chen, G. J. Deng, Q. H. Fan and L. J. Wan, *Chem. – Eur. J.*, 2009, **15**, 9669; (*e*) C. Marie, F. Silly, L. Tortech, K. Mullen and D. Fichou, *ACS Nano*, 2010, **4**, 1288.

2 B. Ilan, G. M. Florio, M. S. Hybertsen, B. J. Berne and G. W. Flynn, *Nano Lett.*, 2008, **8**, 3160.

3 (*a*) M. Yu, N. Kalashnyk, W. Xu, R. Barattin, Y. Benjalal, E. Lægsgaard, I. Stensgaard, M. Hliwa, X. Bouju and A. Gourdon, *et al.*, *ACS Nano*, 2010, **7**, 4097; (*b*) R. Gutzler, S. Lappe, K. Mahata, M. Schmittel, W. M. Heckl and M. Lackinger, *Chem. Commun.*, 2009, 680; (*c*) P. M. Zalake and K. George Thomas, *Langmuir*, 2013, **29**, 2242; (*d*) F. Silly, *J. Phys. Chem. C*, 2012, **116**, 10029.

4 (*a*) L. Xu, X. R. Miao, X. Ying and W. L. Deng, *J. Phys. Chem. C*, 2012, **116**, 1061; (*b*) L. Xu, X. R. Miao, B. Zha, K. Miao and W. L. Deng, *J. Phys. Chem. C*, 2013, **117**, 12707.

5 (*a*) P. Metrangolo and G. Resnati, *Chem. – Eur. J.*, 2001, **7**, 2511; (*b*) S.-K. Noh, J. H. Jeon, W. J. Jang, H. Kim, S. H. Lee, M. W. Lee, J. Lee, S. Han and S.-J. Kahng, *ChemPhysChem*, 2013, **14**, 1177; (*c*) J. Xu, X. Liu, J. K.-P. Ng, T. Lin and C. He, *J. Mater. Chem.*, 2006, **16**, 3540; (*d*) J. K. Yoon, W. j. Son, K. H. Chung, H. Kim, S. Han and S. J. Kahng, *J. Phys. Chem. C*, 2011, **115**, 2297; (*e*) F. Wang, N. Ma, Q. Chen, W. Wang and L. Wang, *Langmuir*, 2007, **23**, 9540.

6 (*a*) R. Gutzler, O. Ivasenko, C. Fu, J. L. Brusso, F. Rosei and D. F. Perepichka, *Chem. Commun.*, 2011, **47**, 9453; (*b*) K.-H. Chung,

J. Park, K. Y. Kim, J. K. Yoon, H. Kim, S. Han and S. J. Kahng, *Chem. Commun.*, 2011, **47**, 11492; (*c*) H. Bertrand, F. Silly, M. P. Teulade-Fichou, L. Tortech and D. Fichou, *Chem. Commun.*, 2011, **47**, 10091.

7 F. Silly, *J. Phys. Chem. C*, 2013, **117**, 20244.

8 M. M. S. Abdel-Mottaleb, G. Gotz, P. Kilickiran, P. Bauerle and E. Mena-Osteritz, *Langmuir*, 2006, **22**, 1443.

9 K. S. Mali, K. Lava, K. Binnemans and S. De Feyter, *Chem. – Eur. J.*, 2010, 14447.

10 (*a*) H. F. Lieberman, R. J. Davey and D. M. T. Newsham, *Chem. Mater.*, 2000, **12**, 490; (*b*) O. Navon, J. Bernstein and V. Khodorkovsky, *Angew. Chem., Int. Ed.*, 1997, **36**, 601.

11 T. T. T. Bui, S. Dahaoui, C. e. Lecomte, G. R. Desiraju and E. Espinosa, *Angew. Chem., Int. Ed.*, 2009, **48**, 3838.